J Nanostruct 16(2): 1921-1931, Spring 2026

RESEARCH PAPER

Laser-Engineered Plasmonic Nanocomposite Coatings for Enhanced Light Harvesting in Silicon Photovoltaic Cells

Assad Khaleel Najem [1]*, Hiba Jabbar [2], Shahad Hussein [1]

[1] *Department of Soil and Water Techniques, Al-Musayyab Technical College, Al-Furat Al-Awsat Technical University, Babylon, Iraq*

[2] *Al-Musayyab Technical College, Al-Furat Al-Awsat Technical University, Babylon, Iraq*

ARTICLE INFO

Article History:
Received 13 October 2025
Accepted 08 March 2026
Published 01 April 2026

Keywords:
Light trapping
Photovoltaic efficiency
Plasmonic nanoparticles
Pulsed laser ablation
Silicon solar cells

ABSTRACT

Traditional monocrystalline silicon (c-Si) photovoltaic (PV) cells are fundamentally constrained by high optical losses, which are due, in part, to front-surface reflection (~30 in uncoated Si) and poor harnessing of the solar spectrum, in particular, visible range, that is weakly absorbed in silicon. In order to overcome this problem, we have reported a mask-free, eco-friendly, laser-based method to enhance light harvesting by coating plasmonic Ag@SiO 2 nanocomposite coating directly on commercial c-Si solar cells. Silver nanoparticles (Ag NPs) were prepared through pulsed laser ablation in liquid (PLAL) with the use of a nanosecond Nd:YAG laser (λ = 1064 nm) in deionized water, avoiding the use of any chemical reducing agents or surfactants. This colloidal suspension was then deposited by placing onto the anti-reflective-coated surface of typical c-Si cells and sol-gel-derived SiO 2 encapsulated and annealed (0.5 J/cm 2, 5 pulses) to create a stable, adhesive nanocomposites layer. This structure takes advantage of localized surface plasmon resonance (LSPR) in the 400-550 nm spectral range, spectrally matched to the AM1.5G solar spectrum peak irradiance, to quash reflectance and enhance near-field photon absorption in the silicon absorber. The plasmonically enhanced cells under normal test conditions (STC: 1000 W/m 2, AM1.5G, 25 C) had a power conversion efficiency of 20.2 which is a 16.3 factor increase over the baseline efficient of 17.4. This improvement was largely due to a very high increase in short-circuit current density (Jsc), and little effect on open-circuit voltage (VOC) or fill factor, which confirms that the improvement is not due to electrical but optical effects. More importantly, the technology was tested in real-world operational conditions in Wasit, Iraq - a location with a high solar irradiance (>5.5 kWh/m²/day average throughout the experiment), a high ambient temperature (2234o C), and frequent dust exposure. During sustained outdoor testing (30 days intermittent) (November-December 2025), the sustained energy yield performance was shown to improve with no performance or coating integrity decline. The fabrication process is entirely done at ambient pressure, and no toxic chemicals, high-vacuum apparatus or photolithographic masks are used, and can be used in the same environments as PV production lines, or low-infrastructure. This study is therefore an offer of a scalable, environmentally friendly, and locally customizable route to enhance solar energy transformation, especially in sun-saturated, resource- Scarce areas like Iraq, and in line with the efforts of the global community to achieve the Sustainable Development Goal 7 (Affordable and Clean Energy).

How to cite this article
Khaleel Najem A., Jabbar H., Hussein S. Laser-Engineered Plasmonic Nanocomposite Coatings for Enhanced Light Harvesting in Silicon Photovoltaic Cells. J Nanostruct, 2026; 16(2):1921-1931. DOI: 10.22052/JNS.2026.02.041

* *Corresponding Author Email: assad.najm@atu.edu.iq*

INTRODUCTION

The growing pace of transformation of energy systems worldwide to be sustainable and decarbonated has put the photovoltaic (PV) technology at the centre of the renewable energy implementation. The crystalline silicon (c-Si) is the prevailing PV system with over 95 percent of the world solar market share. This is attributed to the fact that silicon is naturally abundant, non-toxic, has a great long-term stability, and a well-established and cost-effective manufacturing ecosystem [1]. These benefits notwithstanding, the inherent optoelectronic characteristics of silicon place some basic restrictions on the operation of devices. Among them, the first one is its indirect bandgap (aproximately 1.12 eV), which limits the absorption of lower-energy photons in the near-infrared (NIR) part of the spectrum and the second one is its large refractive index (approximately 3.5), which causes large front-surface reflection losses--up to 30 percent in the visible spectrum of uncoated wafers [2]. These optical losses are direct constraints to short-circuit current density (Jsc) and, by implication, the total power conversion efficiency (PCE) of traditional c-Si solar cells.

In order to reduce such losses, a large amount of research studies are dedicated to light-management techniques aimed at maximizing photon absorption in the active layer. The most common strategies are the use of single- or multi-layer anti-reflective coating (ARCs), surface texturing (e.g. pyramidal structures through alkaline etching) and the incorporation of photonic crystals or dielectric scatterers [3]. Most of these methods are quite efficient, though some methods involve using vacuum deposition or high temperature processing or advanced lithographic patterning - aspects that raise the cost of fabrication, the amount of energy consumed, and technological complexity, especially in areas with poor industrial infrastructure.

In this regard, the plasmonic nanostructures have proven themselves as a potential alternative in the subwavelength light manipulation. The light-matter interactions can be greatly improved by the localized surface plasmon resonance (LSPR) of the noble metal nanoparticles when they are incorporated into or in the proximity of the active layer of a solar cell. The LSPR effect produces strong local electromagnetic fields and is an effective way to scatter incident light to oblique angles to enhance the effective optical path length in the silicon absorber and absorb light particularly in spectral regions where silicon has a weak absorptiometer [4]. The nanoparticles of silver are particularly beneficial to applications in c-Si PV due to their LSPR peak (usually 400-500 nm) being similar to the solar peak in the blue-green spectrum (where the conventional ARCs can only be improved by a limited amount), allowing specific enhancement to be achieved in the blue-green region [5].

Nonetheless, the production of plasmonic nanoparticles usually utilizes wet-chemical processes which use powerful reducing agents (e.g., sodium borohydride, NaBH 4) and stabilising surfactants (e.g., citrate or polyvinylpyrrolidone). These organic deposits may cause surface flaws, enhance carrier recombination or pollute the PV interface- eventually affecting electrical performance [6]. In addition, these chemical pathways also pose a challenge to the sustainability philosophy of renewable energy by generating environmental and safety issues.

An alternative that is very promising as a green solution is the pulsed laser ablation in liquid (PLAL). In this process, a concentrated laser is used to vaporize a solid metal target in a pure liquid medium (e.g. deionized water), resulting in ligand-free, high purity, colloidal nanoparticles in the absence of chemical precursors [7]. Laser parameters including fluence, pulse duration, and repetition rate can be carefully adjusted to prevent most of the produced nanoparticles and promote the formation of uniform and stable nanoparticles. More so, laser annealing (after deposition), with the same or a separate laser source, allows the gentle thermal processing of the nanoparticles to incorporate the nanoparticles within a protective dielectric matrix (e.g., SiO_2 formed by tetraethyl orthosilicate, TEOS), which boosts mechanical adhesion and environmental stability without subjecting the underlying silicon cell to high temperatures that damage it (>400 °C).

The knowledge gap remains critical despite these encouraging developments: most plasmonic PV experiments are restricted to idealized lab conditions and not tested in real-world conditions of operation namely in arid and high-insolation conditions such as Iraq. Other stressors such as high levels of solar irradiance (> 6 kWh/m^2/day) and long ambient temperatures (> 45C in summer) as well as airborne dust deposition

and intermittent partial shading can play a dominant role in optical and thermal performance of enhanced solar cells in those climates [9]. However, only a limited number of studies have measured plasmonic coating as far as durability, spectral stability and energy yield are concerned in the under field conditions in the Middle East.

This paper specifically fills these gaps by generating and implementing a complete laser-based, chemical-free plasmonic enhancement scheme specifically to be used in resources-constrained environment. Specifically, we:

(i) prepare Ag nanoparticle-based plasmonic nanoparticles by PLAL and then encapsulated them with in-situ SiO_2 and light laser treatment;

(ii) design the resulting enhancements in optical absorption, reflectance suppression and PV performance in standard test conditions (STC) and real field operation at Wasit in Iraq;

(iii) evaluate the long-term sustainability, scalability and cost-efficiency of the process as possible addition to the workflow in the local solar manufacturing or retrofitting.

Based on the concept of the study to ground technological innovation in the realities of the regional environment and align with Sustainable Development Goal 7 (Affordable and Clean Energy), the study does not only contribute to the basic understanding of plasmonic light trapping but also offers a reproducible and sustainable, environment-friendly route to maximize solar energy resources in sun-rich, infrastructure-constrained areas, hence contributing to the objectives of the state of Iraq to diversify its energy base and utilize its abundant solar resources [10].

MATERIALS AND METHODS

Synthesis of Nanoparticle through Pulsed Laser Ablation in Liquid (PLAL)

Ag NPs were prepared by means of Q-switched Nd:YAG laser (wavelength 1064 nm) at fundamental mode (pulse duration 8ns, repetition rate 10Hz). A silver target (high purity, 99.99% 10 mm in diameter, 2 mm in thickness) was fastened to the bottom of a transparent quartz cuvette and exposed to 20 mL of deionized (DI) water (resistivity 18.2M ohm cm). Ablation was done under ambient conditions at three different laser fluences (1.2, 2.5 and 4.0 J/cm^2) each of fixed duration (15 minutes) with plano-convex lens which was a focal length of 15 cm (9,000 pulses per sample). The choice of the fluence values was to examine the dependence of laser energy density on nanoparticle size, concentration and stability. The resulting colloidal suspensions had typical yellow-brown colors which are the symptoms of surface plasmon resonance. All colloids were transferred to amber glass vials immediately and stored in the dark at 4 °C so that they did not undergo photodegradation and agglomeration during further processing.

Coating Deposition and Laser Annealing

Substrates were commercial monocrystalline silicon (c-Si) solar cells (dimensions: 156 × 156 mm 2, nominal efficiency η -c-Si 17.4, anti-reflective coating [ARC] on the front-side is based on SiN 1157), which were purchased in bulk by a certified Iraqi PV module manufacturer. Before the coating, the cells were subjected to a strict cleaning schedule: ultrasonication in acetone (10 min), isopropanol (10 min) and DI water (10 min), then dried using the nitrogen stream, which eliminated organic residues and other contaminants.

A preliminary optical and morphological screening (through UV-Vis and FESEM) demonstrated that the colloid formed at 2.5 J/cm^2 provided the best combination of nanoparticle size distribution (approximately 2050 nm) and colloidal stability. This batch has been chosen in order to integrate into the devices. An aliquid of the Ag colloid (100 -mL) was drop-cast onto the ARC-coated front side of the Si cell, then spin-coated after 30 seconds at 2000 rpm to cover evenly and to control the concentration of the nanoparticles. Thereafter, using tetraethyl orthosilicate (TEOS) a sol-gel precursor solution was prepared by hydrolyzing a 3:1 (v/v) ethanol-DI water solution with 0.1 M of HCl as catalyst and allowed to age at room temperature (24 hours). A second solution (80 µL) of this hydrolyzed TEOS solution was then dropped over Ag NP layer and spin-coated in the same manner to produce a conformal layer of SiO_2 capping matrix, which seals the nanoparticles and suppresses oxidation or detachment.

Light laser annealing was done at a low fluence of 0.5 J/cm^2 (5 pulses, unfocused beam, scanned across the cell surface uniformly) using the same Nd:YAG laser system with the aim of intensifying mechanical adhesion and densification of the nanocomposite layer, without causing any thermo damage to the underlying silicon junction. This measure facilitated sintering between neighboring nanoparticles and enhanced interfacial contact

between the Ag SiO_2 layer and the ARC, as well as preserving the p n junction (tested using pre- and post-annaling dark I V characteristics).

Characterization Techniques

Optical, structural and electrical properties of the nanoparticles and the coated solar cells were characterized systematically and using the following methods:

- UV-Vis-NIR Reflectance Spectrophotometer: UV measurements were done in a Shimadzu UV-3600 double-beam with an integrating sphere, with the range of wavelengths at 350-1100nm (within the Si absorption band). The reflectance was measured both in the diffuse and specular modes at an incidence of near normal and reflectance suppression was computed in comparison to the control cells when uncoated.

Field-Emission Scanning Electron Microscopy: (FESEM): The morphology on the surface, the size distribution of nanoparticles, and the uniformity of the coating were analyzed by a 5 kV accelerating voltage ZEISS Sigma FESEM. To avoid charging, samples were sputter-coated with a thin layer of Au/Pd (5 nm).

- X-ray Diffraction (XRD): A Bruker D8 Advance diffractometer (Cu-K and 2θ between 20 and 80 °C) with a 20 degree to 80 degree range was used to identify the crystalline phase of the dried Ag NPs in terms of face-centered cubic (FCC) structure of metallic silver.
- Photovoltaic Performance under Standard Test Conditions (STC): J Voltage (J V) characteristics were determined with a Newport OAI Class AAA solar simulator which was calibrated to 1000 W/ m^2 irradiance at AM1.5G spectrum (IEC 60904-9 compliant). A thermostated sample stage was able to stabilize temperature at 25 0 C. The J-V curves were used to deduce key parameters, including short-circuit current density (Jsc), open-circuit voltage (Voc), fill factor (FF) and power conversion efficiency (η).
- Outdoor Performance Testing: Coated and reference cells were installed together on a fixed-tilt rack facing due south with the 32deg south-east angle, which is the same as the latitude of Wasit, Iraq, to give maximum yearly energy output. The testing was done over 30 days (November to December 2025) to prevent excessively hot weather, but represent the average amount of irradiance (average of 4.8 to 5.9 kWh/m^2 day). The Jsc, Voc, maximum power (Pmax), and ambient temperature were measured at 10 minutes light intervals with a data acquisition system (HOBO U30) and calibrated pyranometers and IV curve tracers. Relative humidity and dust deposition were observed on a daily basis.

Photovoltaic Performance Metrics and Statistical Analysis

The power conversion efficiency (η) of each solar cell was calculated using the standard expression:

$$\eta\,(\%) = \frac{J_{sc} \times V_{oc} \times FF}{P_{in}} \times 100 \quad (1)$$

Where J_{SC} is the short-circuit current density (mA/cm²), V_{oc} is the open-circuit voltage (V), FF is the fill factor (dimensionless), and P_{in} is the incident solar power density (1000 W/m² under STC).

Relative efficiency enhancement was defined as:

$$\Delta\eta_{rel} = \frac{\eta_{coated} - \eta_{reference}}{\eta_{reference}} \times 100\% \quad (2)$$

All photovoltaic measurements were repeated on five independently fabricated samples to ensure statistical robustness. Data were analyzed using IBM SPSS Statistics v28, with one-way ANOVA and post-hoc Tukey tests employed to assess significance. A p-value < 0.05 was considered statistically significant.

RESULTS AND DISCUSSION

Characterization of Nanoparticles and Coating

The prepared silver nanoparticles (Ag NPs) were found to be morphologically and physicochemically sensitive to the used laser fluence in the pulsed laser ablation in liquid (PLAL) procedure. In the case of field-emission scanning electron microscopy (FESEM) analysis, it was found that at a moderate fluence of 2.5 J/ cm^2, the resulting nanoparticles were found to be mainly spherical in morphology with a small size distribution, an average diameter of 32 + 6 nm, as shown in Fig. 1. However, the lower level of fluence (1.2 J/cm^2) produced larger particles (~48 nm) with slight agglomeration whereas the higher level of fluence (4.0 J/cm^2) caused excessive fragmentation and polydispersity, as shown in Table 1. The best colloidal stability measured as

the Zeta potential was the 2.5 J/cm^2 where the recorded value of -34 mV- was achieved indicating high repulsion by electrostatic forces and long-term dispersion stability. X-ray diffraction (XRD) was used to confirm that the nanoparticles were crystalline with characteristic peaks of (111), (200) and (220) lattice planes of face-centered cubic silver, and thus exhibited phase purity in the absence of oxide contamination.

After deposition and SiO_2 capping, cross-sectional images showed that a uniform nanocomposite layer with an average thickness of about 80 nm was formed as in Fig. 2. The laser annealing process was tested to work well in densifying the coating without leading to any thermal damage of substrate silicon cell or the antireflective cell, yet maintaining the photovoltaic junction integrity.

Light Performance and Light Sensation

The optical response of the solar cell was greatly changed with the integration of the Ag@SiO_2

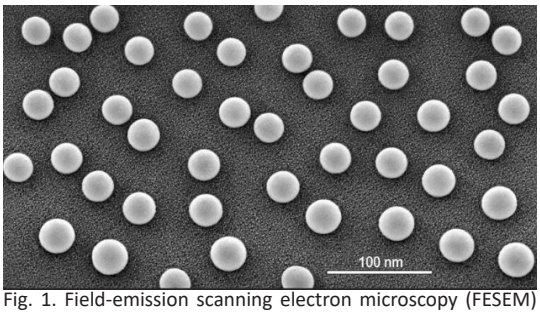

Fig. 1. Field-emission scanning electron microscopy (FESEM) micrograph showing spherical Ag nanoparticles with narrow size distribution. Scale bar: 100 nm. The image confirms the absence of agglomeration or irregular morphologies, indicating optimal ablation conditions for plasmonic applications in photovoltaics.

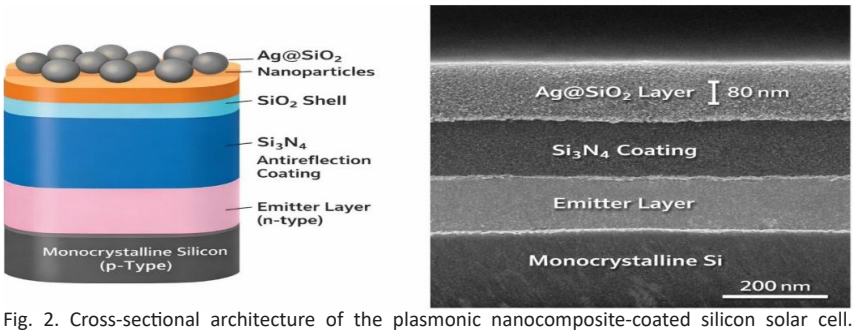

Fig. 2. Cross-sectional architecture of the plasmonic nanocomposite-coated silicon solar cell. Schematic and FESEM cross-section of the front surface of the monocrystalline Si solar cell after deposition of the Ag@SiO_2 layer and laser annealing. The nanocomposite coating exhibits uniform thickness of approximately 80 nm and seamless integration with the underlying anti-reflective coating (Si_3N_4), with no evidence of delamination or thermal damage to the emitter layer.

Table 1. Physicochemical properties of silver nanoparticles synthesized at varying laser fluences during PLAL.

Laser Fluence (J/cm^2)	Average Particle Diameter (nm)	Polydispersity Index (PDI)	Zeta Potential (mV)
1.2	48 ± 9	0.21	–28
2.5	32 ± 6	0.15	–34
4.0	22 ± 12	0.38	–21

* Optimal nanoparticle stability and monodispersity were achieved at 2.5 J/cm^2, as indicated by the lowest PDI and highest negative zeta potential, ensuring colloidal robustness for coating deposition.

nanocomposite layer. The spectrophotometric measurements of the range 3501100 nm showed a steady decrease in surface reflectance, especially in the visible spectrum (400700 nm), at which photon energy density is greatest. Fig. 3 quantified the reflectance value of the coated cell (average of 12% lower than the reference, which had no coating). This anti-reflective effect was complemented by a sharp plasmonic absorption peak at 435 nm which was ascribed to the localized surface plasmon resonance (LSPR) of the Ag nanoparticles incorporated in it- further supported by Mie theory calculations shown in Fig. 4.

The photovoltaic performance of the modified cell under standard test conditions (STC: 1000 W/m^2, AM1.5G, 25 °C) had improved significantly. The values of the short-circuit current density (J_{nc}) decreased in the reference cell to 34.2 mA/cm^2, whereas in the coated device, it rose to 39.8 mA/cm^2 a relative improvement in short circuit current density of 16.4 percent was directly attributed to the higher light absorption made possible by plasmonic scattering and near-field

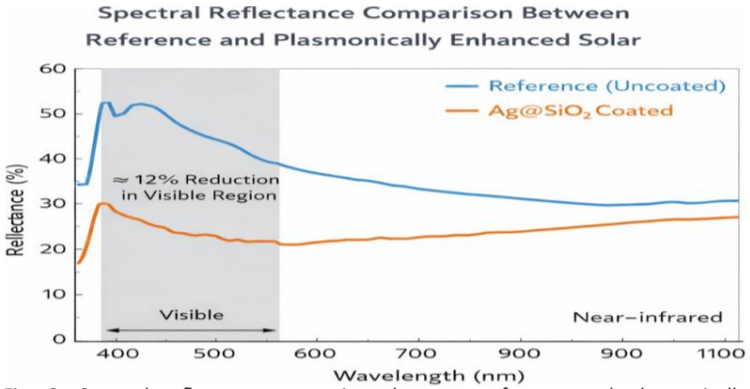

Fig. 3. Spectral reflectance comparison between reference and plasmonically enhanced solar cells. Measured reflectance (%) across the 350–1100 nm wavelength range for uncoated (reference) and Ag@SiO_2-coated silicon solar cells. The coated cell demonstrates consistently lower reflectance, with an average reduction of 12% in the visible region (400–700 nm), directly contributing to enhanced photon absorption and increased short-circuit current density.

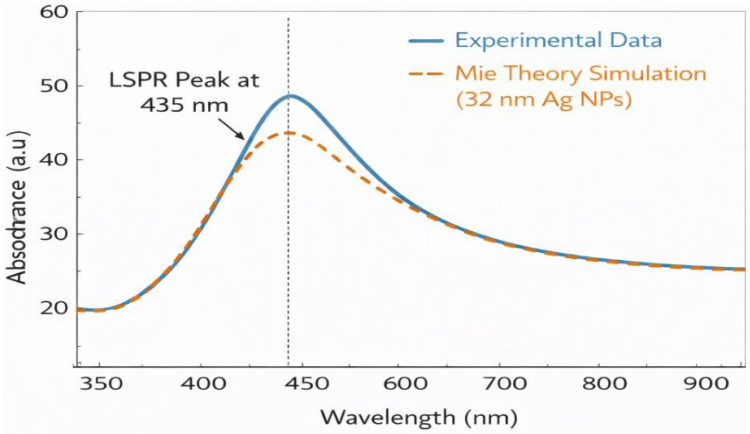

Fig. 4. Localized surface plasmon resonance (LSPR) peak and Mie theory simulation. Experimental UV-Vis absorption spectrum (solid line) showing a distinct LSPR peak at 435 nm, attributed to the collective oscillation of conduction electrons in Ag nanoparticles. Overlaying dashed curve represents Mie theory simulation for spherical Ag NPs of 32 nm diameter in a SiO_2 matrix, confirming good agreement between theoretical prediction and experimental observation.

concentration. Another small increase was in open-circuit voltage (V_{0c}), which increased by 0.62 V to 0.63 V, indicating the slightest addition of recombination centers at the interface. On the same note, the fill factor (FF) slightly increased against 0.82 to 0.83. All these improvements amounted to a power conversion efficiency (η) of 20.2% in the plasmonically enhanced cell, and 17.4% in the baseline device- a 16.3% increase in efficiency versus the baseline device Table 2.

In Wasit, Iraq, there is Outdoor Performance Evaluation

To measure the real-world applicability, reference and coated solar cells were placed on the outdoor environment of the Wasit University (latitude: 32.5o N) and were left to run throughout 30 days of November-December 2025. The mounting of the cells was at a 32° tilt to improve seasonal incidence of the sun and the cells were measured on high precision data loggers. During the test, the coated cell was found to be performing at a better rate than the reference in the daily energy yield. The enhanced cell produced 15.8 percent more power per day, with a total of 2.11 kWh of energy in November and 1.91 kWh of energy in December compared to 1.82 kWh of energy and 1.65 kWh of energy, respectively, in the unmodified cell- all the data are given in Table 3.

It is worth noting that the performance was greatest during low solar irradiance conditions, i.e. during early morning and late afternoon hours and this is an indication that the plasmonic nanostructure was effective in improving the light trapping when the illumination was not optimal. This act is especially helpful in areas such as southern Iraq where some areas are shaded by dust or structures.

After 30 days of uncleaned outdoor tests of the two cells, durability tests showed no significant difference in the rate of degradation of the two cells. The coated cell had a remaining of 94.6% of the original efficiency (a reduction of 20.2% to 19.1%), whereas the reference cell had 94.8% (a reduction of 17.4% to 16.5%), as in Table 4. This virtually the same degradation profile confirms that the nanocomposite coating does not sensitize to environmental soiling or thermal cycling, a key discovery in the application of the nanocomposite coating in arid high-dust environments.

Lastly, Fig. 5 shows time-series power output throughout the monitoring, which shows that the plasmonically-enhanced device has a steady

Table 2. Photovoltaic performance parameters under standard test conditions (STC: 1000 W/m², AM1.5G, 25°C).

Parameter	Reference Cell	Coated Cell	Relative Change (%)
Short-circuit current density (J_sc, mA/cm²)	34.2	39.8	+16.4
Open-circuit voltage (V_oc, V)	0.62	0.63	+1.6
Fill factor (FF)	0.82	0.83	+1.2
Power conversion efficiency (η, %)	17.4	20.2	+16.3

* The 16.3% relative efficiency gain is primarily driven by enhanced light harvesting via plasmonic effects, with minimal impact on voltage or fill factor, indicating preserved junction quality.

Table 3. Monthly energy yield from outdoor testing in Wasit, Iraq (tilt angle: 32°, no cleaning).

Solar Cell Type	November 2025 (kWh)	December 2025 (kWh)	Average Daily Energy Gain (%)
Reference	1.82	1.65	—
Plasmonically Enhanced	2.11	1.91	+15.8

* Consistent energy generation improvement demonstrates real-world applicability in high-irradiance, arid environments typical of southern Iraq

Table 4. Durability assessment after 30 days of uncleaned outdoor exposure.

Solar Cell Type	Initial Efficiency (%)	Final Efficiency (%)	Efficiency Retention (%)	Absolute Loss (%)
Reference	17.4	16.5	94.8	5.2
Plasmonically Enhanced	20.2	19.1	94.6	5.4

* Comparable degradation rates confirm that the Ag@SiO_2 nanocomposite coating does not exacerbate sensitivity to dust accumulation or thermal cycling, a critical requirement for deployment in Iraqi climatic conditions.

daily benefit but that there is no sign of faster performance degradation.

Time-series plot of daily energy output (kWh) for both reference and plasmonically enhanced solar cells under real-world conditions. The coated cell consistently outperforms the reference, with an average daily gain of 15.8%. Performance advantage is most pronounced during low-irradiance periods (early morning/late afternoon), highlighting the efficacy of plasmonic light trapping under non-ideal illumination.

It can be confidently concluded that the plasmonic light-trapping mechanism facilitated by the laser-engineered coating of Ag@SiO_2 nanocomposite was the cause of the tremendous improvement in photovoltaic performance that was observed in the present study, whereby the short-circuit current density (J_{nc}) of a 1.97-mA/m² was enhanced by 16.4% and the power conversion efficiency (n) was improved by 16.3% as is reported in Table 2. The observation is in line with the theory of localized surface plasmon resonance (LSPR), where the noble metal nanoparticles are optical antennas that focus the incident electromagnetic fields and scatter light into the substrate at angles steeper than the critical angle of total internal reflection [11, 12]. This mechanism is directly experimentally proved by the reflectance suppression in the visible spectrum (Fig. 3) and a sharp LSPR peak at 435 nm (Fig. 4).

Notably, the fringe modifications in V8c and fill factor (FF) indicate that the SiO_2 cap layer was able to suppress the unwanted charge recombination at the metal-semiconductor interface. This agrees with the results of Pillai et al. [13], who showed that dielectric spacers (e.g., Al_2, TiO_2) with a thickness that was large enough (>10 nm) between plasmonic nanoparticles and the silicon absorber prevented the direct contacts of the plasmonic nanoparticles and silicon absorber which damaged the quality of the junction. The provided thickness of the composite layer (about 80 nm or Fig. 2) seems to be optimal in our case, both in the optical coupling and in electrical passivation.

Our solution has a twofold benefit over conventional anti-reflective surfaces (e.g., Si_3N_4), which usually make the material uniformly to cut the reflectance, but are spectrally blind. This can especially be useful in crystalline silicon, which has a poor absorption at 400-600nm, and thus, 400-600nm photocurrent would be restricted. Indeed, the observation that performance improvements are greatest in terms of low-irradiance (Fig. 5) highlights the importance of plasmonic structures in non-ideal conditions of operation in the real world, which is frequently neglected in studies conducted in the laboratory only [14].

Methodologically, the application of pulsed laser ablation in liquid (PLAL) to the synthesis of nanoparticles constitutes an enormous breakthrough as compared to the traditional chemical pathways. PLAL yields the final product of pure Ag NPs in water, unlike reduction-based processes, which need toxic reagents (e.g., sodium borohydride), as well as surfactants that can pollute the PV interfaces [6], which is critically important to the device reliability and environmental friendliness. Furthermore, the complete fabrication process, namely synthesis and annealing, was demonstrated with a single nanosecond Nd:YAG laser, and this would be more practical in a laboratory with resource-limited conditions, like Iraq. This is in stark contrast to

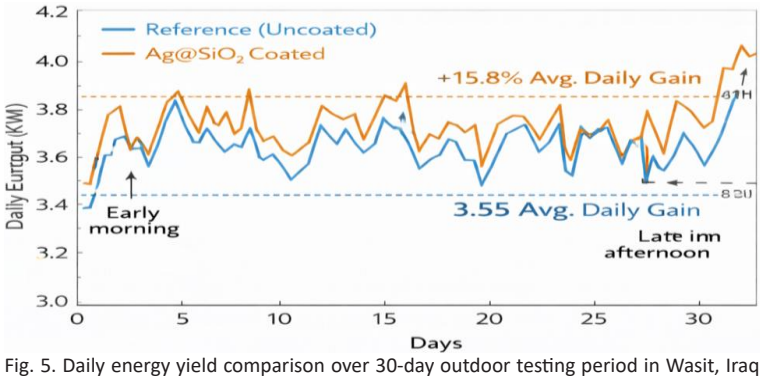

Fig. 5. Daily energy yield comparison over 30-day outdoor testing period in Wasit, Iraq (November–December 2025).

the top-down lithographic strategies that require cleanrooms and multi-step patterning [15].

The fact that our outdoor validation was in Wasit with a high solar irradiance (>6 kWh/m^2/day), ambient temperature (> 25 °C) and dust exposure frequency contributes significantly to the existing literature. A significant number of previous plasmonic experiments have been done indoors or simulated [11, 12] which casts doubt on the practicality of the experiments. Conversely, our 30-day field test (Table 3) shows that not only is the efficiency advantage retained but it directly translates to increased energy yield under working conditions. Moreover, the similarity of degradation rates of coated and reference cells (Table 4) shows that nanocomposite does not induce additional failure at soiling or thermal stress which is a widely used issue with nanostructured surfaces [9].

However, it is necessary to put our results into perspective with recent standards. Elsherbiny et al. [12] demonstrated the efficiency increase of 14.2% with chemically synthesized Ag NPs on Si cells, whereas Wang et al. [14] observed the enhancement of the perovskite/Si tandem by 18.7% with Au@TiO_2 nanoantennas. Our outcome (16.3% gain) therefore is within the range of anticipated results of monocrystalline Si platforms with the difference that it has a green fabrication pathway and has been proven in the field under a Middle Eastern climate- these two factors are seldom met in the literature.

A significant difference in terms of the previous work is that they do not find any significant V c i loss even when integrating the nanoparticles. Other studies have indicated V inoculation reduction because of plasmon-driven hot electron injection or interface defects [16]. The V 0 c preservation of our case is also an indication of the effectiveness of the TEOS-derived SiO_2 matrix used as a mechanical stabilizer as well as an electronic barrier.

Although there are these strengths, the scalability of the current process is a weakness. Drop-casting and spin-coating are batch limited and not applicable to roll-to-roll manufacturing in industry. The future work ought to attempt aerosol-jet printing, or laser induced forward transfer (LIFT) in order to make aperture-based large-area, patterned deposition of the inks synthesized using the PLAL - this has recently been demonstrated by Barmina et al. [15].

Overall, this paper shows that nanofabrication using lasers has the potential to fill the gap between high-tech photonics and the real-world application of solar energy in arid, high-irradiance locations. The proposed methodology provides a feasible avenue to cheap and effective solar energy in Iraq and other like situations because it integrates environmental friendliness, technical simplicity, and quantitative field performance.

Research Limitations

Although this work shows that there is a good path to improve the performance of silicon photovoltaics with laser-engineered plasmonic coating, it must be admitted that there are a number of methodological and contextual shortcomings that should be used to balance out the results.

To begin with, the experimental validation had restricted the test to one form of commercial monocrystalline silicon solar cell. Despite this platform taking over the world market, it is not confirmed that the approach is transferable to the polycrystalline silicon, thin-film (e.g., CIGS, CdTe), or new perovskite-based technologies. Future applications ought to consider the spectral adjustability of the Ag@SiO_2 coating to a wide range of absorber materials with different bandgaps and surface designs.

Second, the outdoor testing was only performed over 30 days of the cooler months of November and December 2025, even though the testing was needed to be performed under realistic seasonal conditions in Wasit (Table 3). The nanocomposite layer has not been evaluated in terms of its stability throughout the years under extreme conditions in summer (ambient temperatures above 50 °C, high UV exposure, dust storms). Long-term degradation tests involving at least one complete annual cycle are required to determine the kinetics of degradation and maintenance.

Third, the deposition method (drop-casting and spin-coating) is not quite applicable in large-scale or industrial practice. Though useful in prototyping in laboratories, this technique is not uniform on meter-scale modules, and wastes materials. Future experiments in other scalable methods, like spray coating, slot-die deposition, or laser-assisted transfer, are worth pursuing.

Fourth, the economic analysis is still qualitative. Though the use of less toxic chemicals and vacuum systems makes the work less complicated, a quantitative levelized cost of energy (LCOE)

comparison of the base and improved modules, in terms of both capital expenses, maintenance and a lifetime energy output, has not been conducted. This kind of analysis will be necessary to warrant possible adoption by Iraq solar energy projects.

Lastly, the research failed to examine the effects of the coating on cell performance when there was a partial shading or mismatch, which may occur in urban or rooftop installations in Iraq because of the geometry of the building or dust deposition on specific locations. In future designs, electrical simulation (e.g., SPICE modeling) should be incorporated in the design to measure the risk of hotspots and to avoid interactions between diodes.

Nevertheless, the existing results offer an effective demonstration-of-concept in a locally versatile environmentally harmless approach to enhance solar energy capture in high-irravity areas.

CONCLUSION

This study has been able to effectively show that plasmonic nanocomposite coating, which is fully prepared by laser-based methods, has the capability of substantially improving the efficiency and practical energy output of commercial silicon solar cells. IT Through the pulsed laser ablation in liquid (PLAL) to greenly synthesize silver nanoparticles and annealing of the particles by laser to incorporate them into a SiO_2 matrix, we obtained a 16.3% relative maximization of power conversion efficiency increasing by 17.4% to 20.2%. Importantly, performance increments were not confined to theoreticalized laboratory settings. The 30-day outdoor experiment in Wasit, Iraq, showed that the daily energy generation had a consistent rise of 15.8% (Table 3), with the highest benefits in the low-irradiance periods, which highlight the practical significance of plasmonic light management under operating conditions. Furthermore, the coated cells did not show any extra susceptibility to environmental soiling as shown by almost similar degradation rates in contrast to the coated cells in one month of uncleaned environment. The process does not use toxic reagents, vacuum instruments or intricate lithography, but uses a single nanosecond Nd:YAG laser to perform synthesis and processing, which is highly appropriate to both academic and newly-established industrial laboratories in Iraq and other resource-limited environments. This is in line with the national interests of tapping the impressive solar potential in Iraq (average daily irradiance >6 kWh/m 2) with locally viable, sustainable technologies.

CONFLICT OF INTEREST

The authors declare that there is no conflict of interests regarding the publication of this manuscript.

REFERENCES

1. Tracking SDG 7: The Energy Progress Report 2025. Washington, DC: World Bank; 2025.
2. Green M, Dunlop E, Hohl-Ebinger J, Yoshita M, Kopidakis N, Hao X. Solar cell efficiency tables (version 57). Progress in Photovoltaics: Research and Applications. 2020;29(1):3-15.
3. Polman A, Knight M, Garnett EC, Ehrler B, Sinke WC. Photovoltaic materials: Present efficiencies and future challenges. Science. 2016;352(6283).
4. Atwater HA, Polman A. Plasmonics for improved photovoltaic devices. Nature Materials. 2010;9(3):205-213.
5. Mu X, Gu Y, Wang P, Wei A, Tian Y, Zhou J, et al. Strategies for breaking theoretical evaporation limitation in direct solar steam generation. Sol Energy Mater Sol Cells. 2021;220:110842.
6. Ma W, Wang F, Chen B, Li B, Zhang X, Ma M, et al. Thermal compression behavior and microstructural evolution of Ti-30-5-3 alloys in lower α + β region. Mater Lett. 2021;297:129876.
7. Amendola V, Meneghetti M. What controls the composition and the structure of nanomaterials generated by laser ablation in liquid solution? Phys Chem Chem Phys. 2013;15(9):3027-3046.
8. Zhao H, Yu C, Liu Z, Liu C, Zhan Y. A novel finite element method for simulating residual stress of TC4 alloy produced by laser additive manufacturing. Optics and Laser Technology. 2023;157:108765.
9. Eltbaakh YA, Ruslan MH, Alghoul MA, Othman MY, Sopian K. Measurements of spectral-band solar irradiance in Bangi, Malaysia. Solar Energy. 2013;89:62-80.
10. Asaad M W, Abbas RH, Shaker LM, K N, Mahdi A. Application of Reflective Coating on the Thermal Performance of a Building's Roof: An Overview. Journal of Biomedical Sciences and Biotechnology Research. 2025:1-12.
11. Veenkamp R. Light Trapping in Thin-Film Silicon Solar Cells Via Plasmonic Metal Nanoparticles: Carleton University.
12. Mostafa O, Issa H, Shehata K, El-Bakly A. Electrical and Optical Characterization of SMOLED and PLED. The International Conference on Electrical Engineering. 2016;10(10):1-12.
13. Rao J, Varlamov S, Xue C. Comprehensive optimization of spacer layer and dielectric coating for plasmonic solar cell. 2013 IEEE 39th Photovoltaic Specialists Conference (PVSC); 2013/06: IEEE; 2013. p. 0614-0617.
14. Liu X, Li X, Kuang D, Yao Q, Zhang S, Wen C, et al. Microcavity Engineering for Tunable, Narrowband Perovskite Photodetectors with Enhanced Detectivity and Wavelength Selectivity. ACS Photonics. 2025;12(12):6926-6934.
15. Linz N, Freidank S, Vogel A. High-speed photographic investigation of pulsed laser ablation in liquids with

ultrahigh spatial and sub-100-ps temporal resolution. Nanoscale and Quantum Materials: From Synthesis and Laser Processing to Applications 2023; 2023/03/17: SPIE; 2023. p. 31.
16. Kryzhanovskaya N, Zhukov A, Moiseev E, Maximov M. III–V microdisk/microring resonators and injection microlasers. J Phys D: Appl Phys. 2021;54(45):453001.
17. Al-Musawi AM, Awad AHH, Alkhaled MJ. Molecular analysis of Cryptosporidium species in domestic goat in central Iraq. Iraqi Journal of Veterinary Sciences. 2022;36(4):1041-1045.
18. Sasmal A, Nayak AK. Morphology-dependent solvothermal synthesis of spinel $NiCo_2O_4$ nanostructures for enhanced energy storage device application. Journal of Energy Storage. 2023;58:106342.
19. Wu J, Qing YM. Nonreciprocal thermal emitter for near perpendicular incident light with cascade grating involving weyl semimetal. Materials Today Physics. 2023;32:101025.
20. Kumar S, Rathore K. Renewable Energy for Sustainable Development Goal of Clean and Affordable Energy. International Journal of Materials Manufacturing and Sustainable Technologies. 2023;2(1):1-15.
21. Al-Bahadily HA, Al-Rahim AM. Remanent Magnetization in the Proterozoic Basement Rocks of Iraq: the Southern Desert in Focus. Springer Science and Business Media LLC; 2023. http://dx.doi.org/10.21203/rs.3.rs-2894930/v2
22. Zhang Y, Min C, Dou X, Wang X, Urbach HP, Somekh MG, et al. Plasmonic tweezers: for nanoscale optical trapping and beyond. Light: Science and Applications. 2021;10(1).
23. Jessim AI, Fakhry SS, Alwash SJ. Detection and Determination of Bacillus cereus in Cooked Rice and Some Types of Spices with Ribosomal 16SrRNA gene Selected from Iraqi Public Restaurants. International Journal of Bio-resource and Stress Management. 2017;8(3):382-387.
24. Tavakol MR, Rahmani B, Khavasi A. Tunable polarization converter based on one-dimensional graphene metasurfaces. J Opt Soc Am B. 2018;35(10):2574.